Dalton Transactions

Cite this: *Dalton Trans.*, 2012, **41**, 12353

www.rsc.org/dalton

COMMUNICATION

Long-lived platinum(II) diimine complexes with broadband excited-state absorption: efficient nonlinear absorbing materials†

Rui Liu,[a] Alexander Azenkeng,[b] Yuhao Li[a] and Wenfang Sun*[a]

Received 12th June 2012, Accepted 24th August 2012
DOI: 10.1039/c2dt31267k

Platinum(II) diimine complexes with naphthalimide substituted fluorenylacetylide ligands are synthesized and characterized. The complexes exhibit long-lived ^{3}ILCT or ^{3}ILCT/^{3}MLCT/^{3}LLCT excited states (τ = ~20–30 μs) and broadband triplet transient absorption in the visible-NIR region. Nonlinear transmission experiments at 532 nm demonstrate that these complexes are efficient nonlinear absorbing materials.

Pt(II) diimine complexes with long-lived excited-states have attracted great attention in recent years because of their potential applications in low-power upconversion,[1] solar energy conversion (*via* photo-induced charge separation),[2] oxygen sensing,[3] and nonlinear optics.[4] For nonlinear optical applications, materials with large excited-state absorption and long-lived excited states are of particular interest. In order to utilize the excited-state absorption, the excited state has to be populated first *via* one-photon or two-photon absorption (TPA) upon excitation. However, the absence of ground-state absorption of the reported Pt(II) diimine complexes above 600 nm prevents accessing the excited state *via* one-photon absorption. To remedy this deficiency, two strategies are proposed: (1) one can modify the molecular structure to bathochromically shift the low-energy absorption band to the desired spectral region; or (2) one can introduce a two-photon absorbing motif to the molecule to populate the excited state *via* TPA. Although both strategies are feasible, the second approach has the advantage of keeping the light color of the material and further enhancing the nonlinear absorption *via* TPA in addition to the excited-state absorption.

Previous studies on Pt diimine arylacetylide complexes demonstrated that the energy of the lowest excited state, namely the metal-to-ligand charge transfer (^{1}MLCT)/ligand-to-ligand charge transfer (^{1}LLCT) states in most cases, decreases when the electron-withdrawing ability of the substituent on the diimine ligand increases or the electron-donating ability of the substituents on the acetylide ligands increases.[5] However, the nature of the lowest excited state of these complexes could be switched from an MLCT/LLCT state to the arylacetylide ligand localized π,π* state or mixed MLCT/LLCT/π,π* when the π-conjugation of the aryl group on the acetylide ligand is extended[6] or a strong electron-withdrawing or donating substituent is introduced on the aryl group.[7] Such a change will not only enhance the ground-state absorption but also influence the excited-state absorption. Therefore, it is critical to choose the appropriate acetylide ligand that can tune the energy of the lowest excited state, but retain the broadband excited-state absorption and long excited-state lifetime of the Pt diimine complexes.

To utilize the 2nd strategy, our group incorporated the benzothiazolyl fluorenylacetylide ligand, which was first applied by the Schanze group in Pt phosphine complexes to show two-photon absorption in the near-IR region,[5d] into Pt bipyridyl complexes. We discovered that the complex containing this ligand not only exhibited remarkable reverse saturable absorption (*i.e.* transmission decreases with increased incident energy due to the stronger excited-state absorption than ground-state absorption) in the visible spectral region but also large TPA in the near-IR region.[4] Therefore, it is a very promising broadband nonlinear absorbing material.

Intrigued by this exciting result, we are pursuing further enhancement of the nonlinear absorption of the Pt(II) diimine acetylide complexes *via* substitution of the benzothiazolyl group by a naphthalimidyl (NI) group. Our rationale for choosing this group is motivated by the seminal work of the Zhao group on a Pt diimine complex with ethynyl naphthalimide ligands, which has an extremely long-lived NI-based lowest triplet excited state (τ_T = 124 μs in MTHF) and broadband excited-state absorption.[3,8] By inserting the fluorene group in the acetylide ligand, we anticipate slightly red-shifting the MLCT/LLCT band to extend the reverse saturable absorption region; meanwhile, fluorene derivatives have been widely used as building blocks for TPA materials.[5d,9] We envision that the TPA of the new complexes could be enhanced. In this work, four Pt(II) complexes containing naphthalimide substituted fluorenylacetylide ligands (**Pt-1**–**Pt-4**, Chart 1) were synthesized and the ground-state and excited-state properties and nonlinear absorption were investigated. **Pt-3** and **Pt-4** lack the low-lying MLCT/LLCT states and are used to compare to the properties of **Pt-1** and **Pt-2**.[8] The branched-alkyl chains were introduced on the ligands to improve the solubility and prevent intermolecular π–π stacking. As

[a]*Department of Chemistry and Biochemistry, North Dakota State University, Fargo, ND 58108-6050, USA. E-mail: Wenfang.Sun@ndsu.edu; Fax: (+1) 701-231-8831*
[b]*Energy and Environmental Research Center, University of North Dakota, Grand Forks, ND 58202-9018, USA*

†Electronic supplementary information (ESI) available: Synthetic scheme, experimental details, characterization data, TDDFT calculation results, UV-Vis absorption and emission spectra and data for the ligands and the Pt(II) complexes in different solvents, ns time-resolved TA spectra of **Pt-1**–**Pt-4**. See DOI: 10.1039/c2dt31267k

reported in this letter, these complexes exhibit long-lived triplet excited states and broadband excited-state absorption, and have been demonstrated to be among the best reverse saturable absorbers for ns laser pulses at 532 nm.

The UV-Vis absorption spectra of the complexes in a CH_2Cl_2 solution (1×10^{-5} mol L^{-1}) are presented in Fig. 1a, and the band maxima and molar extinction coefficients for each complex are compiled in Table 1. The structured absorption bands below 370 nm are assigned to the intraligand (IL) $^1\pi,\pi^*$ transitions of the acetylide ligands. Compared to the $^1\pi,\pi^*$ transitions in their respective ligands (ESI, Fig. S1†), these bands exhibit a bathochromic shift, indicating the delocalization of the ligand-centered molecular orbitals *via* interactions with the Pt dπ orbitals. The broad structureless absorption bands above 370 nm are dominated by the ^{1}ILCT (intra-ligand charge transfer from the ethynylfluorene component to the naphthalimide component) transition,

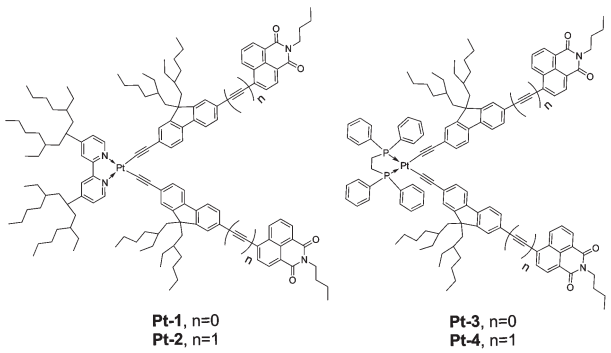

Chart 1 Chemical structures of Pt complexes **Pt-1**–**Pt-4**.

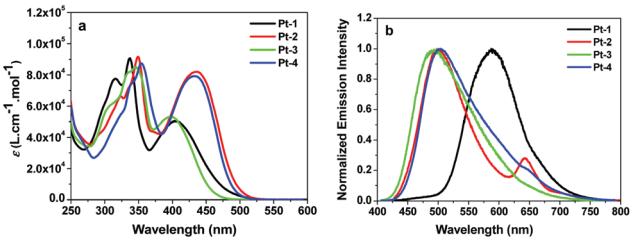

Fig. 1 (a) UV-Vis absorption spectra and (b) normalized emission spectra ($c = 1.0 \times 10^{-5}$ M) of Pt complexes in CH_2Cl_2, 25 °C, λ_{ex} is 417 nm for **Pt-1** and **Pt-2**, 395 nm for **Pt-3** and 419 nm for **Pt-4**.

and mixed with some dπ(Pt) → π*(naphthalimide) and π(C≡C) → π*(C≡C) characters. This assignment is supported by the DFT calculation results for **Pt-1** and **Pt-2** (Fig. 2, Table 2, and ESI, Fig. S2, S3 and Tables S1, S2†) discussed below. Compared to **Pt-3** and **Pt-4**, the visible absorption band in **Pt-1** and **Pt-2** is slightly red-shifted and broadened, which is more salient in **Pt-1** than **Pt-2**. With reference to the DFT calculation results, ^{1}MLCT (dπ(Pt) → π*(bipyridyl))/^{1}LLCT (ligand-to-ligand charge transfer from π(fluorenylacetylide) to π*(bipyridyl)) transitions also contribute to the visible absorption band in **Pt-1**, but not to the band in **Pt-2**. This could explain the longer tail in **Pt-1** that is absent in **Pt-2**. The charge transfer nature of the visible absorption band is reflected by the negative solvatochromic effect (ESI, Fig. S4, S5†). Notably, the tail in complex **Pt-1** is also red-shifted compared to its analogue reported in the literature, which has no fluorene component in the acetylide ligands.[3,8] The red-shifted tail in **Pt-1** and **Pt-2** in the visible region is critical for broadening the reverse saturable absorption spectral region, which requires the population of excited states *via* one-photon absorption.

Density-functional theory (DFT) calculations and time-dependent density functional theory (TDDFT) calculations were performed for complexes **Pt-1** and **Pt-2** in CH_2Cl_2 in order to understand the nature of the ground and excited electronic states (Fig. 2, Table 2, and ESI, Fig. S2, S3 and Tables S1, S2†). The calculation results indicate that the HOMO and HOMO − 1 orbitals are essentially fluorenylacetylide and Pt metal based for both **Pt-1** and **Pt-2**, while the LUMO is almost exclusively π* (naphthalimide) based for **Pt-2**, and delocalized on π*(naphthalimide) and π*(bipyridine) for **Pt-1**. The electron density distributions on the LUMO + 1 are similar to that of the LUMO for **Pt-2**, with the dominant contribution from the π*(naphthalimide); but the LUMO + 2 is dominated by the π*(bipyridyl). For **Pt-1**, LUMO + 2 resembles that of LUMO, with the dominant contribution from the π*(bipyridine) and π*(naphthalimide); but the LUMO + 1 is exclusively localized on the π* (naphthalimide).

The TDDFT calculation results show that the 1st excited state for **Pt-1** occurs at 375 nm, which has the dominant contributing configuration involving the HOMO → LUMO and HOMO → LUMO + 2 orbital pairs; while the 2nd excited state that involves the HOMO − 1 → LUMO and HOMO − 1 → LUMO + 2 orbital pairs as the dominant configurations appears at 361 nm. For **Pt-2**, the 1st excited state involving the HOMO → LUMO

Table 1 Photophysical parameters of **Pt-1**–**Pt-4**

	λ_{abs}/nm ($\varepsilon/10^4$ L mol^{-1} cm^{-1})[a]	λ_{em}/nm (τ_{em}/ns; Φ_{em})[b]	λ_{T1-Tn}/nm (τ_{TA}/μs; $\varepsilon_{T1-Tn}/10^4$ M^{-1} cm^{-1}; Φ_T)[d]	σ_0 [e]/10^{-18} cm^2	σ_{ex} [f]/10^{-18} cm^2	σ_{ex}/σ_0	$\Phi_T\sigma_{ex}/\sigma_0$
Pt-1	337 (9.10), 404 (5.04)	589 ([c], 0.012)	535 (21.6, 6.24,0.11)	0.78	256	328	37.4
Pt-2	349 (9.17), 436 (8.20)	500 ([c], 0.051), 646 ([c])	565 (29.6, 6.89, 0.091)	1.54	242	157	14.2
Pt-3	345 (8.52), 398 (5.32)	494 (90, 0.118)	535 (31.2, 5.77, 0.084)	—	220	—	—
Pt-4	353 (8.75), 433 (7.94)	503 (80, 0.122)	565 (27.3, 6.19, 0.083)	0.52	191	367	30.2

[a] Electronic absorption band maxima and molar extinction coefficients in CH_2Cl_2 at room temperature. [b] Room temperature emission band maxima and decay lifetimes measured in CH_2Cl_2 at a concentration of 1×10^{-5} mol L^{-1}. A degassed aqueous solution of $[Ru(bpy)_3]Cl_2$ ($\Phi_{em} = 0.042$, excited at 436 nm) was used as the reference. [c] Too weak to be measured. [d] ns TA band maximum, triplet extinction coefficient, triplet excited-state lifetime and quantum yield. Measured in CH_3CN. SiNc in C_6H_6 was used as the reference (ε_{590} = 70 000 L mol^{-1} cm^{-1}, $\Phi_T = 0.20$). [e] Ground-state (σ_0) absorption cross section at 532 nm, measured in CH_3CN. [f] Excited-state absorption cross section (σ_{ex}) at 532 nm, measured in CH_3CN.

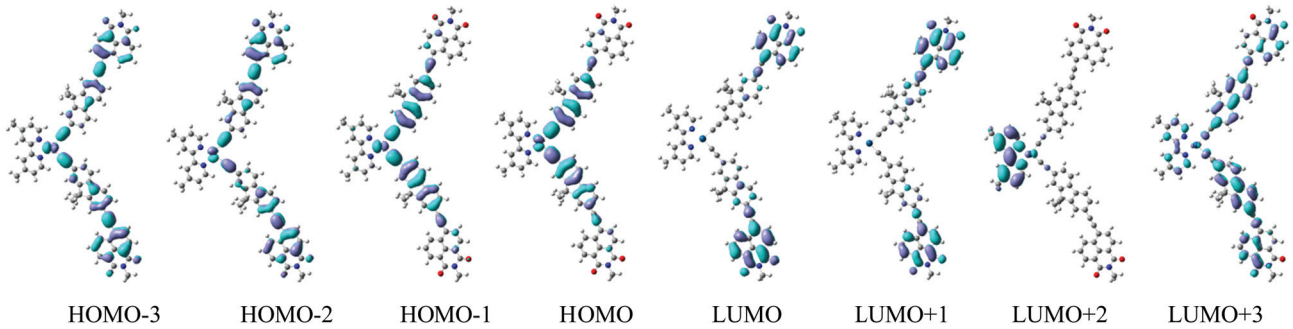

Fig. 2 Contour plots of the four highest occupied molecular orbitals (HOMOs) and four lowest unoccupied molecular orbitals (LUMOs) for **Pt-2** in CH_2Cl_2.

Table 2 Excitation energies (eV), wavelengths (nm), oscillator strengths, main contributing transitions, and the associated configuration coefficients of five low-lying electronic states of complex **Pt-2** in CH_2Cl_2 obtained at the CAM-B3LYP/LANG631//B3LYP/LANG631 level of theory. All calculations include corrections due to solvent effects using the PCM model

	Excitation energy				
S_n	eV	nm	f	Main contributing transitions	Coefficient of main contributing configuration
1	3.02	409	3.362	HOMO → LUMO	0.40
				HOMO − 1 → LUMO + 1	0.35
2	3.08	402	0.966	HOMO − 1 → LUMO	0.40
				HOMO → LUMO + 1	0.37
3	3.35	370	0.021	HOMO → LUMO + 2	0.58
4	3.47	356	0.224	HOMO − 1 → LUMO + 2	0.56
5	3.83	324	0.175	HOMO → LUMO + 3	0.35
				HOMO − 2 → LUMO	0.28
				HOMO − 3 → LUMO + 1	0.28

and HOMO − 1 → LUMO + 1 orbital pairs as the dominant configurations appears at 409 nm; while the 2nd excited state (involving the HOMO − 1 → LUMO and HOMO → LUMO + 1 orbital pairs as the dominant configurations) occurs at 402 nm. According to the electron density distributions on HOMO − 1, HOMO, LUMO, LUMO + 1, and LUMO + 2, the 1st and 2nd excited states should be predominantly attributed to ^{1}ILCT/^{1}MLCT/^{1}LLCT transitions for **Pt-1** and ^{1}ILCT transition for **Pt-2**, which correspond to the broad, structureless absorption band between 360 nm and 500 nm for **Pt-1** and the 380–520 nm band for **Pt-2**, respectively. It is noted that the UV-Vis absorption band maxima and the values predicted by calculations are generally consistent with each other and the trend for **Pt-1** and **Pt-2** is also in line with the experimental result. This supports our initial assignment of the absorption bands discussed in the preceding paragraph.

To understand the excited state characteristics that are closely related to nonlinear absorption, emission of **Pt-1**–**Pt-4** in a degassed CH_2Cl_2 solution was studied. Excitation of these complexes at their respective visible charge-transfer band at room temperature results in structureless blue-to-orange luminescence (Fig. 1b). The emission of **Pt-2**, **Pt-3**, and **Pt-4** exhibits relatively small Stokes shifts and short lifetimes (<5 ns). The emission energy is quite similar to the fluorescence from their respective acetylide ligands (ESI, Fig. S6†). In addition, similar to that observed in the ligand, the emission exhibits a positive solvatochromic effect (ESI, Fig. S7–S11†). Therefore, the observed emission for **Pt-2**, **Pt-3**, and **Pt-4** can be assigned to the ^{1}ILCT fluorescence from the acetylide ligand. This assignment is also consistent with the nature of the lowest singlet excited state of **Pt-2** described above. However, **Pt-2** exhibits an additional emission band at 646 nm, which is quite sensitive to oxygen quenching (ESI, Fig. S12†). Considering the large Stokes shift and sensitivity to oxygen quenching, this band can be ascribed to phosphorescence from the ^{3}ILCT excited state. In contrast, **Pt-1** exhibits a broad structureless emission at 589 nm, which is sensitive to oxygen quenching and shows a positive solvatochromic effect (ESI, Fig. S13†). With reference to the TDDFT calculation results for **Pt-1**, which ascribes the lowest singlet excited state of **Pt-1** to be ^{1}ILCT/^{1}MLCT/^{1}LLCT, and with the assumption that the singlet/triplet splitting may not be large, we attribute the emission of **Pt-1** to the ^{3}ILCT/^{3}MLCT/^{3}LLCT excited states. It is noted that the nature of the emitting state for **Pt-1**–**Pt-4** is significantly altered compared to their analogue reported in the literature without the fluorene component in the acetylide ligands, which possesses long-lived $^3\pi,\pi^*$ phosphorescence from the acetylide ligand.[3,8]

Transient difference absorption (TA) spectroscopy is a critical technique to understand the excited-state absorption. One can not only identify the spectral region where excited-state absorption is stronger than ground-state absorption from the spectral feature, but also obtain the lifetime of the excited state from the decay of the transient absorption. Fig. 3a displays the triplet TA spectra of the Pt complexes at the zero time delay in a degassed CH_3CN solution. **Pt-1**–**Pt-4** exhibit similar spectral features, with bleaching occurring below 450 nm and broad absorption bands in the visible to the NIR region. Similar to that observed in their UV-Vis absorption spectra, the absorption bands in **Pt-2**

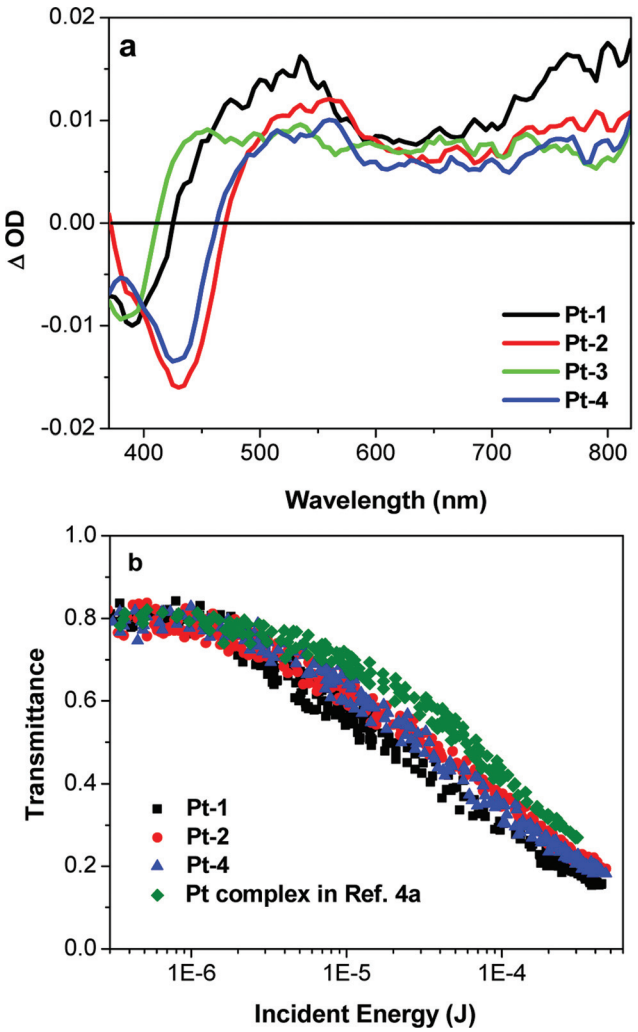

Fig. 3 (a) Triplet transient difference absorption spectra of Pt complexes at zero delay after the 355 nm pulsed-laser excitation in a degassed CH_3CN solution, A_{355} = 0.4 in a 1 cm cuvette; (b) nonlinear transmission curves for Pt complexes in CH_2Cl_2 for 4.1 ns laser pulses at 532 nm. The radius of the beam waist at the focal point was ~96 μm. The linear transmission for all samples was adjusted to 80% in a 2 mm cuvette.

and **Pt-4** are obviously red-shifted compared to those in **Pt-1** and **Pt-3** due to the extended π-conjugations in the acetylide ligand. The lifetimes obtained from the decay of the TA (Table 1) are ~20–30 μs, which are remarkably different from the emission lifetimes and are much longer than that for a typical triplet metal-to-ligand charge-transfer excited state. This indicates that the excited state giving rise to the TA is from the triplet excited state. Considering the nature of the lowest singlet excited state for **Pt-1** and **Pt-2** discussed earlier, which is ^{1}ILCT/^{1}MLCT/^{1}LLCT and ^{1}ILCT, respectively, and assuming the singlet and triplet excited state splitting is not large, the triplet excited state giving rise to the observed TA spectra for **Pt-1** and **Pt-2** could be ^{3}ILCT/^{3}MLCT/^{3}LLCT and ^{3}ILCT, respectively. This notion is consistent with the assignment of the lowest triplet excited state for these two complexes based on the phosphorescence of **Pt-1** and **Pt-2**. The involvement of ^{3}MLCT/^{3}LLCT characters in **Pt-1** but not in **Pt-2** is reflected by the salient red-shift of the visible absorption band and the stronger NIR absorption band in **Pt-1** compared to those in **Pt-3**, which is in line with that observed from the respective UV-Vis absorption spectra. For **Pt-2**, the TA feature is essentially identical to that of **Pt-4**. Thus the transient absorbing excited state for **Pt-2** and **Pt-4** is assigned to the ^{3}ILCT state. The same attribution is applied to **Pt-3** considering the similar TA features between **Pt-3** and **Pt-2** and **Pt-4**. These assignments are supported by the similar TA features of **Pt-2**–**Pt-4** to those of their corresponding ligands **1-L** and **2-L** in CH_3CN (ESI, Fig. S26, S27†), in which the excited state giving rise to the TA is believed to be the ^{3}ILCT state (the lowest triplet excited state in polar solvents). It should be pointed out that the lifetimes for **Pt-1**–**Pt-4** are much longer than that for the Pt complex bearing benzothiazolyl fluorenylacetylide ligands reported by our group earlier.[4a] The long-lived triplet excited state and the broadband excited-state absorption imply that reverse saturable absorption (RSA) could occur from these complexes in the visible spectral region.

Reverse saturable absorption (RSA) is a nonlinear absorption phenomenon that the absorptivity of the molecule increases with increased incident energy due to stronger excited-state absorption with respect to the ground-state absorption. In order for RSA to occur, the molecule has to exhibit larger excited-state absorption cross-section (σ_{ex}, which describes the probability of a molecule at a lower excited state to absorb one photon of the excitation light to be populated to a higher excited state, and is proportional to the excited-state molar extinction coefficient *via* equation $\sigma = 2303\varepsilon/N_A$) than the ground-state absorption cross section (σ_0, *i.e.* the probability of a molecule at the ground state to absorb one photon to be populated to the singlet excited state). Namely, the ratio of σ_{ex}/σ_0 has to be larger than 1; and the larger the σ_{ex}/σ_0 ratio, the stronger the RSA. To demonstrate the RSA, a nonlinear transmission experiment at 532 nm was carried out in CH_2Cl_2 solutions (Fig. 3b) using ns laser irradiation for **Pt-1**, **Pt-2**, and **Pt-4**. **Pt-3** has no ground-state absorption at 532 nm and thus the excited state cannot be populated *via* one-photon absorption at this wavelength. As a result, RSA cannot be observed and the nonlinear transmission experiment was not carried out for **Pt-3**. The concentration of each complex solution was adjusted to obtain a linear transmission of 80% in a 2 mm cuvette. To evaluate the effect of the naphthalimide substituent compared to the benzothiazole substituent on the nonlinear absorption, a Pt complex bearing benzothiazolyl fluorenylacetylide ligands reported by our group earlier[4a] was also measured under the same conditions. With increased incident energy, the transmission of these Pt complexes decreases drastically, which clearly manifests the RSA at 532 nm. The strength of the RSA follows this trend: **Pt-1** > **Pt-4** > **Pt-2** > Pt complex in ref. 4*a*. Among these, **Pt-1** exhibits the strongest RSA, with the transmission decreasing to 15% when the incident energy reaches ~440 μJ. The RSA of these complexes at 532 nm is stronger than the Pt complex bearing benzothiazolyl fluorenylacetylide ligands reported by our group earlier.[4a]

Because all of the complex solutions have the same linear transmission to guarantee the same population at the singlet excited state upon excitation, the observed nonlinear transmission difference should be attributed to the different ratios of the excited-state absorption cross section to that of the ground-state (σ_{ex}/σ_0). In addition, because RSA of ns laser pulses are

dominated by the triplet excited-state absorption, the triplet excited-state quantum yield (Φ_T) should also play a role. Therefore, the key parameter that determines the RSA of ns laser pulses is the $\Phi_T\sigma_{ex}/\sigma_0$ value of a molecule. The ground-state absorption cross sections at 532 nm for these complexes are deduced from the ε values obtained from their UV-Vis absorption using the conversion equation $\sigma = 2303\varepsilon/N_A$, where N_A is the Avogadro constant. The triplet excited-state absorption cross sections at 532 nm are estimated from the ΔOD at zero time delay of the ns TA spectrum and the ε_{T1-Tn} at the TA band maximum (Table 1). The results are compiled in Table 1. The $\Phi_T\sigma_{ex}/\sigma_0$ values for these complexes at 532 nm follow this trend: **Pt-1** > **Pt-4** > **Pt-2**. The stronger RSA of **Pt-1** than **Pt-2** is a result of the extended π-conjugation in the acetylide ligands, which red-shifts both the ground-state and excited-state absorption spectra. Consequently, the ground-state absorption cross section at 532 nm increases while the triplet excited-state absorption decreases, leading to the reduced ratio of $\Phi_T\sigma_{ex}/\sigma_0$ and decreased RSA in **Pt-2** compared to that in **Pt-1**. The stronger RSA of **Pt-4** than **Pt-2** is mainly attributed to the reduced σ_0 at 532 nm for **Pt-4**, leading to a larger ratio of $\Phi_T\sigma_{ex}/\sigma_0$ for **Pt-4** than for **Pt-2**. It is worth noting that the estimated σ_{ex}/σ_0 values for these complexes at 532 nm are much larger than most of the reverse saturable absorbers reported in the literature at 532 nm (see ESI, Table S6†).[10] (It should be noted that comparison of the bulk RSA of different molecules reported in the literature that are measured under different experimental conditions is meaningless because different concentrations, thicknesses of samples, different wavelengths or experimental setups will affect the RSA results drastically. A better way to evaluate the performance of a reverse saturable absorber is to compare the intrinsic molecular parameter σ_{ex}/σ_0.) Although the σ_{ex}/σ_0 values for **Pt-1**, **Pt-2** and **Pt-4** are somewhat smaller than those for the Pt complex with benzothiazolyl fluorenylacetylide ligands,[4a] the values reported in this work are estimated values using different methods from that reported previously for the Pt complex with benzothiazolyl fluorenylacetylide ligands.[4a] Because the estimated σ_{ex} values using the method briefed in this work are generally smaller than the σ_{ex} values obtained *via* fitting of the *Z*-scan data using a five-level model (which is the case for obtaining the σ_{ex} values for the Pt complex with benzothiazolyl fluorenylacetylide ligands),[4a] the σ_{ex} values and the σ_{ex}/σ_0 and $\Phi_T\sigma_{ex}/\sigma_0$ ratios reported in this paper for **Pt-1**, **Pt-2** and **Pt-4** are the bottom-line values for these complexes. The true values will be reported later by conducting *Z*-scan measurements and fitting the *Z*-scan data using a five-level model.[4a] Nevertheless, the much longer lifetimes of **Pt-1**, **Pt-2** and **Pt-4** could compensate for the somewhat smaller σ_{ex}/σ_0 values, leading to the observed stronger RSA for these complexes than the Pt complex bearing benzothiazolyl fluorenylacetylide ligands.[4a] From the comparison of the σ_{ex}/σ_0 values listed in Table S6†, the RSA of **Pt-1**, **Pt-2** and **Pt-4** should be much stronger than the other reverse saturable absorbers reported in the literature if the RSA experiments are carried out under identical conditions. Therefore, they are among the best reverse saturable absorbers for ns laser pulses at 532 nm. Moreover, these complexes could potentially exhibit large two-photon absorption in the near-IR region considering the charge-transfer nature of the lowest excited state of these complexes (this will be studied and reported in the near future). They are thus very promising broadband nonlinear absorbing materials as well.

In conclusion, the Pt(II) diimine complexes bearing naphthalimide substituted fluorenylacetylide ligands exhibit strong ^{1}ILCT or mixed ^{1}ILCT/^{1}MLCT/^{1}LLCT absorption bands in the visible spectral region, as well as long-lived ^{3}ILCT or ^{3}ILCT/^{3}MLCT/^{3}LLCT excited states (τ = ~20–30 μs) and broadband triplet TA in the visible-NIR region. Upon ns laser pulse irradiation at 532 nm, strong RSA occurs. Thus, these Pt complexes are among the most promising nonlinear absorbing materials. Moreover, their long-lived triplet excited states make them potential candidates for upconversion, oxygen sensing, and photovoltaic applications.

Notes and references

1 (*a*) Y. Liu, Q. Li, J. Zhao and H. Guo, *RSC Adv.*, 2012, **2**, 1061; (*b*) H. Sun, H. Guo, W. Wu, X. Liu and J. Zhao, *Dalton Trans.*, 2011, **40**, 7834; (*c*) L. Huang, L. Zeng, H. Guo, W. Wu, W. Wu, S. Ji and J. Zhao, *Eur. J. Inorg. Chem.*, 2011, **2011**, 4527.

2 (*a*) M. Hissler, J. E. McGarrah, W. B. Connick, D. K. Geiger, S. D. Cummings and R. Eisenberg, *Coord. Chem. Rev.*, 2000, **208**, 115; (*b*) J. E. McGarrah, Y.-J. Kim, M. Hissler and R. Eisenberg, *Inorg. Chem.*, 2001, **40**, 4510; (*c*) S. Suzuki, R. Sugimura, M. Kozaki, K. Keyaki, K. Nozaki, N. Ikeda, K. Akiyama and K. Okada, *J. Am. Chem. Soc.*, 2009, **131**, 10374.

3 H. Guo, S. Ji, W. Wu, W. Wu, J. Shao and J. Zhao, *Analyst*, 2010, **135**, 2832.

4 (*a*) W. Sun, B. Zhang, Y. Li, T. M. Pritchett, Z. Li and J. E. Haley, *Chem. Mater.*, 2010, **22**, 6384; (*b*) T. M. Pritchett, W. Sun, B. Zhang, M. J. Ferry, Y. Li, J. E. Haley, D. M. Mackie, I. I. I. W. Shensky and A. G. Mott, *Opt. Lett.*, 2010, **35**, 1305.

5 (*a*) M. Hissler, W. B. Connick, D. K. Geiger, J. E. McGarrah, D. Lipa, R. J. Lachicotte and R. Eisenberg, *Inorg. Chem.*, 2000, **39**, 447; (*b*) T. J. Wadas, R. J. Lachicotte and R. Eisenberg, *Inorg. Chem.*, 2003, **42**, 3772; (*c*) C. E. Whittle, J. A. Weinstein, M. W. George and K. S. Schanze, *Inorg. Chem.*, 2001, **40**, 4053; (*d*) J. E. Rogers, J. E. Slagle, D. M. Krein, A. R. Burke, B. C. Hall, A. Fratini, D. G. McLean, P. A. Fleitz, T. M. Cooper, M. Drobizhev, N. S. Maka-rov, A. Rebane, K. Y. Kim, R. Farley and K. S. Schanze, *Inorg. Chem.*, 2007, **46**, 6483.

6 I. E. Pomestchenko, C. R. Luman, M. Hissler, R. Ziessel and F. N. Castellano, *Inorg. Chem.*, 2003, **42**, 1394.

7 Z. Li, E. Badaeva, D. Zhou, J. Bjorgaard, K. D. Glusac, S. Killina and W. Sun, *J. Phys. Chem. A*, 2012, **116**, 4878.

8 H. Guo, M. L. Muro-Small, S. Ji, J. Zhao and F. N. Castellano, *Inorg. Chem.*, 2010, **49**, 6802.

9 (*a*) B. A. Reinhardt, L. L. Brott, S. J. Clarson, A. G. Dillard, J. C. Bhatt, R. Kannan, L. Yuan, G. S. He and P. N. Prasad, *Chem. Mater.*, 1998, **10**, 1863; (*b*) K. D. Belfield, D. J. Hagan, E. W. Van Stryland, K. J. Schafer and R. A. Negres, *Org. Lett.*, 1999, **1**, 1575; (*c*) M. H. V. Werts, S. Gmouh, O. Mongin, T. Pons and M. Blanchard-Desce, *J. Am. Chem. Soc.*, 2004, **126**, 16294; (*d*) P. N. Day, K. A. Nguyen and R. Pachter, *J. Phys. Chem. B*, 2005, **109**, 1803.

10 (*a*) F. Guo, W. Sun, Y. Liu and K. Schanze, *Inorg. Chem.*, 2005, **44**, 4055; (*b*) P. Shao, Y. Li, J. Yi, T. M. Pritchett and W. Sun, *Inorg. Chem.*, 2010, **49**, 4507; (*c*) Z. Ji, Y. Li, T. M. Pritchett, N. S. Makarov, J. E. Haley, Z. Li, M. Drobizhev, A. Rebane and W. Sun, *Chem.–Eur. J.*, 2011, **17**, 2479; (*d*) B. Zhang, Y. Li, R. Liu, T. M. Pritchett, A. Azenkeng, J. E. Haley, A. Ugrinov, Z. Li, M. R. Hoffmann and W. Sun, *Chem.–Eur. J.*, 2012, **18**, 4593; (*e*) Y. Li, T. M. Pritchett, J. Huang, M. Ke, P. Shao and W. Sun, *J. Phys. Chem. A*, 2008, **112**, 7200; (*f*) T. M. Pritchett, W. Sun, F. Guo, B. Zhang, M. J. Ferry, J. E. Rogers-Haley, W. Shensky III and A. G. Mott, *Opt. Lett.*, 2008, **33**, 1053; (*g*) W. Sun, Y. Li, T. M. Pritchett, Z. Ji and J. E. Haley, *Nonlinear Optics, Quantum Optics: Concepts in Modern Optics*, 2010, **40**, 163; (*h*) Y. Song, G. Fang, Y. Wang, S. Liu and C. Li, *Appl. Phys. Lett.*, 1999, **74**, 332; (*i*) J. Si, M. Yang, Y. Wang, L. Zhang, C. Li, D. Wang, S. Dong and W. Sun, *Appl. Phys. Lett.*, 1994, **64**, 3083.